DESY 04-142

Low x particle spectra in the Modified Leading Logarithm Approximation

S. Albino, B. A. Kniehl, and G. Kramer

II. Institut für Theoretische Physik, Universität Hamburg,

Luruper Chaussee 149, 22761 Hamburg, Germany

(Dated: August 9, 2004)

Abstract

We show that the higher moments of the evolution obtained from the Modified Leading Logarithm Approximation may be regarded as spurious higher order terms in perturbation theory, and that neglecting them leads to a good description of the data around and above the peak in $\xi = \ln(1/x)$. Furthermore, we use this study of the moments to show that at high energy the Limiting Spectrum with Local Parton-Hadron Duality may also be derived from the Modified Leading Logarithm Approximation without any non-perturbative assumptions.

arXiv:hep-ph/0408112 v1 9 Aug 2004

I. INTRODUCTION

The perturbative QCD approximation is consistent with a wide range of data. However, there are two formal limitations on the predictive power of this approximation. Firstly, perturbative QCD is incomplete in that it does not describe the physics of hadrons entirely. Secondly, the perturbation series becomes singular when any of the virtual and real quarks and gluons (collectively called partons) in a process has a configuration of energy and momenta whose "energy scale" E, a quantity whose definition cannot be precisely defined and which is integrated over in virtual loops, is as small as $\Lambda_{\rm QCD}$, the fundamental scale of QCD which determines the scale at which non-perturbative effects become important. For virtual partons, these two problems are related through the factorization theorem, which states that the dominant (leading twist) contribution to a hadronic process at high energy is given by a convolution over dimensionless kinematic variables of process dependent quantities describing those partons with E greater than the factorization scale Q, which is fixed, with process independent quantities which describe both asymptotic hadrons and partons with $E < Q$. The former quantities and the Q dependences of the latter quantities are calculable in perturbation theory in a given factorization scheme, which defines E, provided that Q is sufficiently much larger than $\Lambda_{\rm QCD}$. Processes with real partons are calculable in perturbative QCD provided one performs a physical sum over these particles.

In the fixed order approach, where the perturbation series is calculated to a finite order, the perturbative series for a given partonic process can become divergent in certain regions of phase space. Fortunately, the terms that cause the divergences in a given region are often calculable to all orders, with the formal sum of all terms of a given class being free of divergences in that region and forming the term of a given order in a new series.

The hadronic and low E partonic components of processes involving the inclusive production of hadrons are contained in fragmentation functions (FF's), which describe the probability of transition from a high E parton a to a low E hadron h. In this case it is valid to identify E with the transverse momentum of each parton. The cross section for a given process is obtained by convoluting the FF's with the partonic cross sections (the coefficient functions) over the ratio z of the hadron's longitudinal momentum to that of the parton. The FF's at one value of Q can be calculated perturbatively from those at another value Q_0 by convoluting with the evolution matrix, which describes the probabili-

ties of transition from a parton at Q to another at Q_0, and which is obtained in terms of the perturbatively calculable splitting functions by solving the DGLAP equation. However, the series for the splitting functions breaks down as $z \to 0$ due to terms which behave in this limit like $(\alpha_s^n/z)\ln^{2n-1-m} z$, where $m = 1, ..., 2n-1$ labels the class of terms. (Terms which behave like α_s^n are classified as $m = 2n$.) These logarithms must be resummed before the fixed order splitting functions are valid at small z. Since the cross section at hadronic momentum fraction $x = 2p/\sqrt{s}$, where p is the momentum of the produced hadron h and $\sqrt{s}$ is the centre-of-mass energy, depends on the FF's over the range $x \leq z \leq 1$, such a resummation is required to describe the cross section at small x. Resummation of the leading ($m = 1$) and subleading ($m = 2$) logarithms, which appear at leading order, is obtained via the Modified Leading Logarithmic Approximation (MLLA) [1] (for reviews see [2, 3]). Since the coefficient functions are non-singular as $z \to 0$, and the quark FF's are proportional to the gluon FF in the MLLA, the cross section at low x is then proportional to the MLLA evolved gluon FF.

There is some freedom to choose the MLLA evolution due to the next-to-MLLA error. The evolution given by the analytic solution to the MLLA differential equation [4] is well behaved for $Q_0 = O(\Lambda_{\rm QCD})$, which may imply that the two limitations on perturbation theory to describe hadronic physics that were mentioned at the beginning of this section are too stringent. The first limitation may be weakened by introducing the Local Parton-Hadron Duality (LPHD) hypothesis [5], which states that the distribution of partons below a certain energy scale in sufficiently inclusive processes is similar to the distribution of hadrons, up to the number of particles actually produced (the multiplicity). This implies that the initial hadronic fragmentation function is proportional to the partonic fragmentation function for $Q_0 = O(\Lambda_{\rm QCD})$. The second limitation may be weakened by assuming that partons with $E = O(\Lambda_{\rm QCD})$ may be described by perturbation theory (after resumming with the MLLA). Together with the LPHD, the particular choice $Q_0 = \Lambda_{\rm QCD}$ in the MLLA evolution gives the Limiting Spectrum [5]. The only free parameters are the initial normalisation and $\Lambda_{\rm QCD}$, which can be fitted to the data. A good fit to the data over the whole range of $\xi = \ln(1/x)$ can be achieved, however only if the evolution of the normalization is modified. In [6] an additional component not provided by the MLLA was added to the normalization, whereas in [7] a different normalization was fitted for each value of $\sqrt{s}$. Otherwise $\Lambda_{\rm QCD}$ obtained in this approach is consistent with that of other analyses.

In our recent work [8], we studied the MLLA evolution without using strong assumptions such as the LPHD or the validity of the Limiting Spectrum, nor modifying the MLLA evolution itself. Using an initial scale $Q_0 \gg \Lambda_{\rm QCD}$ and a parameterized function for the initial gluon FF, we achieved a good description of the charged hadron cross section data for ξ up to and around the peak, and obtained values of $\Lambda_{\rm QCD}$ close to those in the literature. Beyond the peak the MLLA evolution turned out not to be sufficient to describe the data. The theoretical curves exhibited a second bump after the first peak, not seen in the data, which have a characteristic Gaussian shape around the first peak. Such a problem cannot be solved by modifying the MLLA normalization.

It is expected that the fixed order approach with double and single logarithms resummed with the MLLA should give a good description of the small to large ξ data, and therefore, if fixed order corrections are not included, one has to consider qualitatively what effect the fixed order prediction at small ξ has on the MLLA prediction at large ξ. In fact, the MLLA formally improves the description of the Mellin transform of the cross section for small $|\omega|$, where ω is defined in Eq. (1), rather than the cross section itself at large ξ. Fixed order calculations indicate that the large ξ region has rather little dependence on the large $|\omega|$ region.

It is the purpose of this paper to consider the features of the data that the MLLA can describe, and thereby modify the MLLA evolution in order to improve the description of the large ξ behaviour of the spectra without spoiling the description around the peak. We start in Section II by considering the moments of the cross section, since these quantities depend very little on the large $|\omega|$ behaviour of the evolution and the parameterization of the initial gluon FF, and can be easily extracted from the data. We then derive our approach for improving the large ξ description. In Section III, we compare the predictions of this approach with the experimental data at large ξ. In Section IV, we study the effect of imposing the limits of the LPHD and Limiting Spectrum on our approach. Finally, in Section V, we present our conclusions.

II. EVOLUTION OF MOMENTS IN THE MLLA

In this Section we outline the features of the MLLA that will be important for the derivation of our main result. More details can be found in our previous publication [8],

however, to make our formulae here more transparent we will refrain from using the variables $Y = \ln(Q/Q_0)$ and $\lambda = \ln(Q_0/\Lambda_{\rm QCD})$ and write Q and Q_0 explicitly.

The MLLA is believed to describe the energy dependence of cross sections for hadron production in the region for which $\alpha_s \ll 1$ and $|\omega| = O(\sqrt{\alpha_s})$, where ω replaces the variable x in the Mellin transform

$$f_\omega = \int_0^\infty d\xi \exp[-\omega\xi] x f(x). \tag{1}$$

In this limit the cross section is proportional to the gluon FF $D(x,Q)$ at the conventional choice of factorization scale $Q = \sqrt{s}/2$. The dependence of the gluon FF on Q in Mellin space takes the simple form

$$D_\omega(Q) = E_\omega(\alpha_s(Q), \alpha_s(Q_0)) D_\omega(Q_0), \tag{2}$$

where $D_\omega(Q_0)$ is non-perturbative, while E_ω is determined in terms of the gluon splitting function $\gamma_\omega(\alpha_s)$,

$$E_\omega(\alpha_s(Q), \alpha_s(Q_0)) = \exp\left[\int_{Q_0}^{Q} d\ln\mu \ \gamma_\omega(\alpha_s(\mu))\right]. \tag{3}$$

From the MLLA, the double and single logarithmic contribution to $\gamma_\omega(\alpha_s)$ reads

$$\gamma_\omega(\alpha_s) = \frac{1}{2}\left(-\omega + \sqrt{\omega^2 + 4\gamma_0^2}\right) + \frac{\alpha_s}{2\pi}\left[b\frac{\gamma_0^2}{\omega^2+4\gamma_0^2} - \frac{a}{2}\left(1 + \frac{\omega}{\sqrt{\omega^2+4\gamma_0^2}}\right)\right] + O\left(\left(\frac{\alpha_s}{\omega}\right)^3\right), \tag{4}$$

where $\alpha_s(Q)$ is calculated at one loop order and depends on the number of flavours N_f, $\gamma_0^2 = 4N_c\alpha_s/(2\pi)$ for $N_c = 3$ colours, $a = 11N_c/3 + 2N_f/(3N_c^2)$ and $b = 11N_c/3 - 2N_f/3$. As is usual in applications of the MLLA, we choose $N_f = 3$. Eq. (4) is an expansion of γ_ω in α_s/ω keeping α_s/ω^2 fixed. The first line is of order α_s/ω, and is obtained from the Double Logarithm Approximation (DLA), while the second is the MLLA correction of $O\left((\alpha_s/\omega)^2\right)$. The $O\left((\alpha_s/\omega)^3\right)$ error is the unknown next-to-MLLA correction. Since Eq. (4) reduces to a finite series in $\sqrt{\alpha_s}$ at $\omega = 0$, the MLLA should also be a good approximation in the region $|\omega|, \sqrt{\alpha_s} \ll 1$ if the next-to-MLLA corrections in this region are of higher order in $\sqrt{\alpha_s}$.

One is interested in determining what improvements the MLLA makes to the cross section in x space. This quantity can be obtained from the inverse Mellin transform, given by

$$xD(x,Q) = \frac{1}{2\pi i}\int_C d\omega \exp[\omega\xi] D_\omega(Q), \tag{5}$$

where the contour C may be taken to be a straight line from $\omega = \omega_0 - i\infty$ to $\omega = \omega_0 + i\infty$, where ω_0 is real and to the right of all singularities in $D_\omega(Q)$. Actually, the small ξ dependence of $D(x,Q)$ is largely determined by E_ω at large $|\omega|$, which is described by the fixed order result. Coincidentally, the MLLA also leads to a good description of the small ξ region, since γ_ω in Eq. (4) becomes negative at large $|\omega|$ like the fixed order result. On the other hand, as $\xi \to \infty$ the contribution from the $|\omega| < O(\sqrt{\alpha_s})$ region becomes increasingly relevant, and may eventually become dominant since the evolution of the cross section calculated in the fixed order approach falls off rapidly at large $|\omega|$ due to the $-\ln|\omega|$ behaviour of the anomalous dimensions to all orders. However, γ_ω in Eq. (4) only approaches a constant, $-a\alpha_s/(2\pi)$, at large $|\omega|$, so it cannot be expected that this approach to the MLLA gives a good description at large ξ. There is no guarantee that there exists some suitable choice for the large $|\omega|$ behaviour of $D_\omega(Q_0)$ which can remedy this problem with the evolution.

Therefore we require an evolution which approximates the MLLA well in the $|\omega| < O(\sqrt{\alpha_s})$ region and which falls off sufficiently fast at large $|\omega|$ such that the small $|\omega|$ region gives the dominant contribution to the cross section at large ξ. For this purpose we will study the MLLA in terms of the moments K_n of the gluon FF, where

$$K_n(Q) = \left(-\frac{d}{d\omega}\right)^n \ln D_\omega(Q)\bigg|_{\omega=0}, \tag{6}$$

since the first few moments (n finite) depend very little on the behaviour of the evolution at large $|\omega|$. The K moments completely determine $D_\omega(Q)$, since Eq. (6) may be inverted using Taylor's Theorem to give, formally,

$$\ln D_\omega = \sum_{n=0}^{\infty} \frac{K_n(-\omega)^n}{n!}. \tag{7}$$

Note that the K moments may be expressed in terms of the normalized ξ moments, $\langle \xi^n \rangle$, which from Eq. (1) can be calculated using

$$\langle \xi^n \rangle = \frac{1}{D_0}\left(-\frac{d}{d\omega}\right)^n D_\omega\bigg|_{\omega=0}. \tag{8}$$

From Eqs. (2) and (6), the moments of the gluon FF evolve as

$$K_n(Q) = K_n(Q_0) + \Delta K_n(\alpha_s(Q), \alpha_s(Q_0)), \tag{9}$$

where ΔK_n is defined to be the nth K moment of the evolution E_ω, and so the K moments have the additional advantages that their MLLA evolution is independent of $D_\omega(Q_0)$ and

that they each evolve independently of one another. This definition of ΔK_n together with Eq. (3) implies

$$\Delta K_n(\alpha_s(Q),\alpha_s(Q_0)) = \int_{Q_0}^{Q} d\ln\mu \left(-\frac{d}{d\omega}\right)^n \gamma_\omega(\alpha_s(\mu))\Big|_{\omega=0}. \tag{10}$$

Explicitly, Eqs. (4) and (10) for $n \geq 1$ give

$$\Delta K_n(\alpha_s(Q),\alpha_s(Q_0)) = \alpha_s^{-\frac{n+1}{2}}(Q)\left(C_n^{(0)} + C_n^{(1)}\alpha_s^{\frac{1}{2}}(Q) + O\left(\alpha_s\right)\right) - \left\{\alpha_s(Q) \leftrightarrow \alpha_s(Q_0)\right\}, \tag{11}$$

where the $O\left(\alpha_s\right)$ error refers to unknown next-to-MLLA corrections, while the $C_n^{(0,1)}$ are completely determined and are presented in [9] for the first few values of n. In fact, for $n \geq 3$ and odd, $C_n^{(0)} = 0$. Eq. (11) also applies for $n = 0$, but ΔK_0 also contains a term proportional to $\ln\alpha_s$.

For small $|\omega|$, $E_\omega(\alpha_s(Q),\alpha_s(Q_0))$ may be approximated by

$$\ln E_\omega(\alpha_s(Q),\alpha_s(Q_0)) = \sum_{n=0}^{M} \frac{\Delta K_n(\alpha_s(Q),\alpha_s(Q_0))(-\omega)^n}{n!} \tag{12}$$

with M finite. This corresponds to evolving the moments K_n for $n \leq M$ exactly as in the full unexpanded case, but fixing the remaining K moments to be equal to $K_n(Q_0)$. Since the coefficient $C_n^{(0)}$ in Eq. (11) for n even is positive when $n/2$ is odd and negative when $n/2$ is even, then in the region where the imaginary part of ω is large, if $M \geq 2$ and even, Q and Q_0 are large and $Q_0 < Q$, we obtain the fast decrease

$$E_\omega \to \exp\left[-\frac{\left|\Delta K_M \omega^M\right|}{M!}\right]. \tag{13}$$

If M is odd, the Mth term in Eq. (12) just produces an oscillation, in which case the replacement $M \to M-1$ in Eq. (13) must be made.

It remains to be found whether Eq. (12) agrees well with the approach of Eqs. (2) to (4) in the whole region $|\omega| < O(\sqrt{\alpha_s})$. In the extreme case $|\omega| = O(\sqrt{\alpha_s})$, Eq. (11) implies

$$\omega^n \Delta K_n = O\left(\alpha_s^{-\frac{1}{2}}\right), \tag{14}$$

so that all terms in the series in Eq. (12) become of similar magnitude. Such a series may still converge, or oscillate with an average value equal to the unexpanded result. In any case, we see that the accuracy of Eq. (12) to reproduce the MLLA contribution to the cross section cannot be reliably determined in Mellin space. Therefore we will try to determine

what the suppression of higher moments means in x space. For this purpose, it will be convenient to work with the moments N, $\overline{\xi}$, σ^2 and κ_n for $n = 3, ..., \infty$, defined by

$$\begin{aligned} N &= D_0, \qquad \overline{\xi} = \langle \xi \rangle, \qquad \sigma^2 = \langle \left(\xi - \overline{\xi}\right)^2 \rangle, \qquad \kappa_3 = \frac{\langle \left(\xi - \overline{\xi}\right)^3 \rangle}{\sigma^3}, \\ \kappa_4 &= \frac{\langle \left(\xi - \overline{\xi}\right)^4 \rangle}{\sigma^4} - 3, \qquad \kappa_n = \frac{\langle \left(\xi - \overline{\xi}\right)^n \rangle}{\sigma^n} \qquad (n \geq 5). \end{aligned} \tag{15}$$

Note that κ_3 is often written as s and κ_4 as k. From Eqs. (6) and (8), these moments are related to the K moments by

$$K_0 = \ln N, \qquad K_1 = \overline{\xi}, \qquad K_2 = \sigma^2, \qquad K_n = \sigma^n \kappa_n \qquad (n \geq 3). \tag{16}$$

To obtain an expression for some function $D(x)$ in terms of the κ_n, we first make the replacement $y = i\omega\sigma$ in Eq. (5), which yields

$$x D(x) = \frac{N}{\sigma\sqrt{2\pi}} \exp\left[-\frac{\delta^2}{2}\right] R(\delta, \{\kappa_n\}), \tag{17}$$

where $\delta = (\xi - \overline{\xi})/\sigma$ and the real quantity R is given by

$$R(\delta, \{\kappa_n\}) = \frac{e^{\delta^2/2}}{\sqrt{2\pi}} \int_{-\infty}^{\infty} dy \exp\left[\sum_{n=3}^{\infty} \kappa_n \frac{(-iy)^n}{n!}\right] \exp\left[iy\delta - \frac{y^2}{2}\right]. \tag{18}$$

Note that R is equal to unity when all the κ_n vanish. We therefore see that a function depends on its moments K_n for $n \geq 3$ only through the ratios $\kappa_n = K_n/\sigma^n$. To calculate Eq. (17) to a given accuracy when the κ_n are small, we expand the κ_n-dependent exponential in Eq. (18) in powers of the κ_n up to the required accuracy and perform the integral for each term. R is then rewritten as an exponential of the form

$$R = \exp\left[\sum_{i=0}^{\infty} A_i \delta^i\right], \tag{19}$$

where each A_i vanishes when all the κ_n vanish. Now suppose the κ_n are sufficiently small such that it is valid to expand the A_i in the κ_n for $n \leq M$ up to some finite order, and neglect the moments κ_n for $n > M$. In this case $\ln R$ as a series in δ will terminate at some finite order, hence the argument of the exponential in Eq. (19) is not an expansion in δ, since the approximation is valid even if δ is of $O(1)$. For example, including the complete contribution from all terms of $O(s)$, $O(k)$, $O(s^2)$, $O(k^2)$, $O(sk)$, $O(\kappa_5)$ and $O(\kappa_6)$ in $\ln R$

gives

$$
\begin{aligned}
xD(x) = \frac{N}{\sigma\sqrt{2\pi}} \exp\Bigg[& \frac{1}{8}k - \frac{1}{2}s\delta - \frac{1}{4}(2+k)\,\delta^2 + \frac{1}{6}s\delta^3 + \frac{1}{24}k\delta^4 \\
& - \frac{5}{24}s^2 + \frac{1}{12}k^2 - \frac{1}{48}\kappa_6 + \left(\frac{1}{8}\kappa_5 - \frac{2}{3}sk\right)\delta + \left(\frac{1}{2}s^2 - \frac{1}{3}k^2 + \frac{1}{16}\kappa_6\right)\delta^2 \\
& + \left(-\frac{1}{12}\kappa_5 + \frac{7}{12}sk\right)\delta^3 + \left(-\frac{1}{8}s^2 + \frac{7}{48}k^2 - \frac{1}{48}\kappa_6\right)\delta^4 \\
& + \left(\frac{1}{120}\kappa_5 - \frac{1}{12}sk\right)\delta^5 + \left(-\frac{1}{72}k^2 + \frac{1}{720}\kappa_6\right)\delta^6 \Bigg].
\end{aligned}
\tag{20}
$$

We now return to hadron production cross sections in the MLLA. In x space, Eq. (2) becomes

$$
xD(x,Q) = \int_x^1 \frac{dz}{z}\frac{x}{z} E\left(\frac{x}{z}, \alpha_s(Q), \alpha_s(Q_0)\right) zD(z,Q_0), \tag{21}
$$

where $E(z, \alpha_s(Q), \alpha_s(Q_0))$ is the inverse Mellin transform of $E_\omega(\alpha_s(Q), \alpha_s(Q_0))$. From Eq. (16), the κ moments of $zE(z, \alpha_s(Q), \alpha_s(Q_0))$, $\kappa_n^E(\alpha_s(Q), \alpha_s(Q_0))$, obey (omitting arguments for brevity)

$$
\kappa_n^E = \frac{\Delta K_n}{(\Delta K_2)^{\frac{n}{2}}}. \tag{22}
$$

We may use Eq. (11) to expand $\kappa_n^E(\alpha_s(Q), \alpha_s(Q_0))$ as a series in $\alpha_s(Q)$ keeping $\alpha_s(Q_0)$ fixed, giving

$$
\kappa_n^E(\alpha_s(Q), \alpha_s(Q_0)) \propto {\alpha_s}^{\frac{n-2}{4}}(Q)\left[1 + O\left(\alpha_s^{\frac{1}{2}}(Q)\right)\right]. \tag{23}
$$

Therefore we may treat the κ_n^E as small, in which case E takes the form of Eq. (17),

$$
zE(z, \alpha_s(Q), \alpha_s(Q_0)) = \frac{N^E}{\sigma^E\sqrt{2\pi}} \exp\left[-\frac{\delta^{E2}(z)}{2}\right] R^E(\delta^E(z), \{\kappa_n^E\}), \tag{24}
$$

where $\delta^E(z) = (\ln(1/z) - \overline{\xi}^E)/\sigma^E$. Eq. (23) and the discussion after Eq. (19) show that when $\ln R^E$ is expanded in $\alpha_s(Q)$ while $\delta^E(z)$ is fixed, the higher moments serve only to contribute spurious higher order terms to this series. Such terms give a large theoretical error, since they contribute unstable "noise", as can be seen by performing the evolution on a smooth function. Discarding these terms gives an evolution in which the higher moments of the gluon FF are fixed with respect to Q, in other words Eq. (12).

Similarly, the κ moments of $D(x,Q)$ obey

$$
\kappa_n(Q) = \frac{K_n(Q_0) + \Delta K_n(\alpha_s(Q), \alpha_s(Q_0))}{[K_2(Q_0) + \Delta K_2(\alpha_s(Q), \alpha_s(Q_0))]^{\frac{n}{2}}}. \tag{25}
$$

TABLE I: Simultaneous fit of $\Lambda_{\rm QCD}$ and the moments $\ln N$, $\overline{\xi}$, σ^2, K_3 and K_4 at $Q_0 = 14/2$ GeV to the same moments of the data from [6]. $\chi^2_{\rm DF} = 3.7$.

$\ln N$	$\overline{\xi}$	σ^2	K_3	K_4	$\Lambda_{\rm QCD}$ (MeV)
2.00	2.09	0.40	0.05	-0.19	411 ± 36

At sufficiently large Q, $\Delta K_n(\alpha_s(Q), \alpha_s(Q_0)) \gg K_n(Q_0)$, so that, from Eqs. (22) and (25), $\kappa_n(Q)$ may be approximated by $\kappa_n^E(\alpha_s(Q), \alpha_s(Q_0))$, and hence may be treated as small. Thus if Q_0 is sufficiently large, $xD(x, Q_0)$ may be parameterized as a distorted Gaussian around the average value of ξ.

III. FITTING TO DATA

Since the evolution of the first few K moments is independent of the approach used (e.g. the approach of Eqs. (2) to (4) or the approach of Eq. (12)) and the parameterization of the non-perturbative input, the ability of the MLLA to describe the data in principle can be determined by comparison to the moments of the data, assuming that fixed order corrections can be neglected. We perform a single fit of $\Lambda_{\rm QCD}$ and the initial K_n with $Q_0 = 14/2$ GeV to the K_n of the experimental data at various $\sqrt{s}$ by setting $Q = \sqrt{s}/2$ and evolving in the MLLA as in Eq. (10). We use the moments calculated in [6], which are presented in the form N, $\overline{\xi}$, σ^2, s and k, from which we extract the first 5 K moments, and their errors are obtained by differentiating and adding in quadrature. The results are shown in Table I and Fig. 1. The error on $\Lambda_{\rm QCD}$ in Table I and in all other tables in this paper is obtained by inverting the correlation matrix, which is identified with the matrix of second derivatives. In Fig. 1, we see that the first 3 moments are fitted very well, however there is a marginal disagreement of K_3 and K_4 with the data which may result from either an inability of the MLLA to describe these higher K moments or from the inaccuracy involved in obtaining these moments from the experimental data, in which case the true experimental error would be larger than that shown. We also perform a fit directly to the basis of moments used in [6], and found no significant change in the values of the initial parameters, and the theoretical curves for s and k deviated seriously from the data below $\sqrt{s} \approx 25$ GeV.

These results strongly suggest that there exists some approach to applying the MLLA and

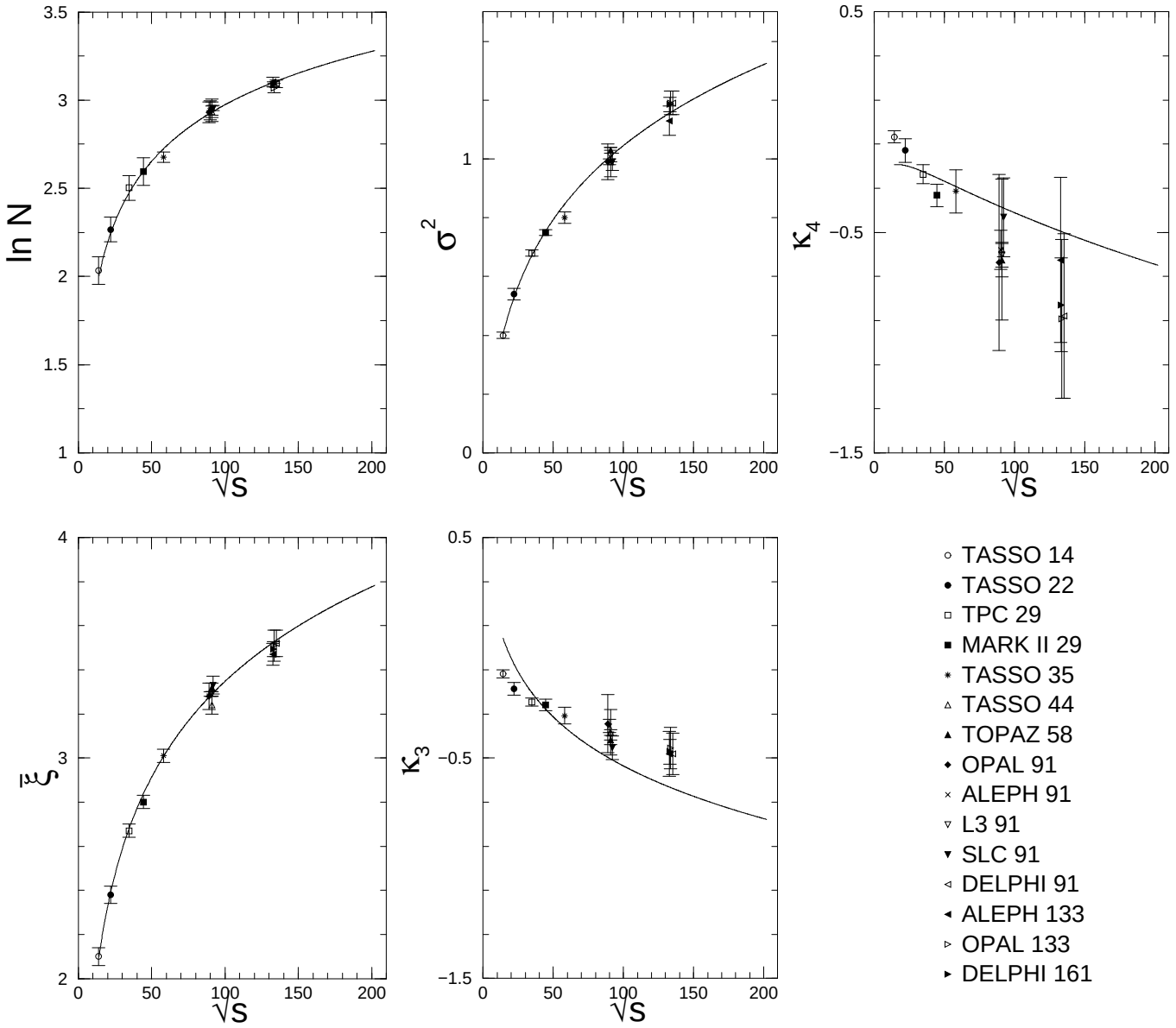

FIG. 1: Simultaneous fit of the initial moments and $\Lambda_{\rm QCD}$ to all of the experimental data moments calculated in [6], by evolving the moments in the MLLA.

some parameterization of the non-perturbative components that gives a good description of the data over a large range in ξ. In the following three subsections we perform fits directly to the data points at different ξ using various approaches. In Subsection III A, we evolve the moments, place them in a distorted Gaussian and compare with the data at different ξ. In Subsections III B and III C, we evolve in Mellin space using Eq. (12), with two different parameterizations of the non-perturbative input: In Subsection III B we parameterize the initial distribution $xD(x,Q_0)$ such that its higher moments are exactly

zero but the remaining moments are left as free parameters, while in Subsection III C we parameterize the initial distribution as a distorted Gaussian (the first two lines of Eq. (20)) so that the higher moments are small. In order to avoid the small ξ region, where fixed order effects are important and where the data have a high accuracy, we follow [7] and use only those data for which

$$\xi > 0.75 + 0.33 \ln(\sqrt{s}), \tag{26}$$

but impose no upper limit in ξ on the data.

A. Evolution of moments as distorted Gaussian parameters

While the data tend to follow the shape of a distorted Gaussian well, the distorted Gaussian evolved with the approach of Eqs. (2) to (4) does not — in [8], the theoretical curves exhibited two bumps. Therefore we constrain the evolved $xD(x,Q)$ to follow a distorted Gaussian,

$$xD(x,Q) = \frac{N'}{\sigma'\sqrt{2\pi}} \exp\left[\frac{1}{8}k' - \frac{1}{2}s'\delta' - \frac{1}{4}\left(2+k'\right)\delta'^2 + \frac{1}{6}s'\delta'^3 + \frac{1}{24}k'\delta'^4\right], \tag{27}$$

with $\delta' = (\xi - \overline{\xi}')/\sigma'$, where the parameters N', $\overline{\xi}'$, σ', k' and s' depend on Q. Since these parameters are approximately equal to the corresponding unprimed quantities defined in Eq. (15), we choose their Q dependences to be the same, i.e. that obtained from Eqs. (10) and (16). By comparing $xD(x,Q)$ calculated in this way with the data at different ξ and $\sqrt{s}$, we fit the initial $K'_n(Q_0) = K'_n$ for $n \leq 5$, as well as $\Lambda_{\rm QCD}$, with the choice $Q_0 = 14/2$ GeV. A similar approach was applied in [7], however the Limiting Spectrum formulae for the moments were used, and $\Lambda_{\rm QCD}$, the peak position of the data and the normalisation of the data for each $\sqrt{s}$ were fitted. We use TASSO data at $\sqrt{s}$ =14, 22, 35 and 44 GeV [10], TPC [11] and MARK II [12] data at 29 GeV, TOPAZ data at 58 GeV [13], ALEPH [14], DELPHI [15], L3 [16], OPAL [17] and SLD [18] data at 91 GeV, ALEPH [19] and OPAL [20] data at 133 GeV, DELPHI data at 161 GeV [21], OPAL data at 172, 183 and 189 GeV [22] and OPAL data at 202 GeV [7]. The results are shown in Table II, and some of the data with the corresponding fitted theoretical curves are shown in Fig. 2. (In all plots in this paper, each curve is shifted up from the curve below by 0.8 for clarity.) The fit is excellent around the peak and above, but poor below the peak region, where fixed order effects are

TABLE II: Simultaneous fit of $\Lambda_{\rm QCD}$ and the moments $\ln N'$, $\overline{\xi}'$, σ'^2, K_3' and K_4' at $Q_0 = 14/2$ GeV to the data in x space by evolving them in the MLLA and placing them in a distorted Gaussian. $\chi^2_{\rm DF} = 2.4$.

$\ln N'$	$\overline{\xi}'$	σ'^2	K_3'	K_4'	$\Lambda_{\rm QCD}$ (MeV)
2.41	2.07	0.91	-0.58	-0.66	59 ± 4

important. In particular, the curves show that the MLLA alone predicts the evolution of the normalization very well at large ξ, in contrast to other analyses. This procedure has a

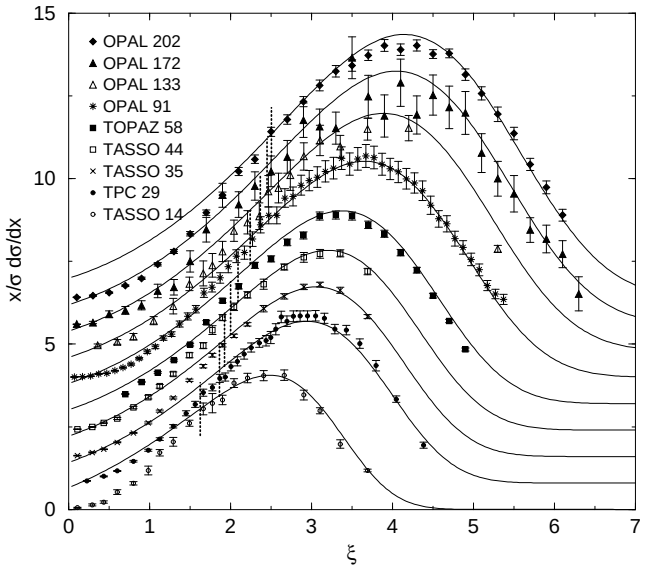

FIG. 2: Global fit by using a distorted Gaussian in which the moments are evolved in the MLLA. The lower limits of the data used, given by Eq. (26), are indicated by vertical dotted lines. Each curve is shifted up by 0.8 for clarity.

number of features that differ from that used in [8]. The evolution used there coincidentally shares similar properties at large $|\omega|$ with the fixed order result, and hence a good fit was obtained with the data below the peak while a large disagreement was found above the peak. However, no properties of the evolution used for the fit of Table II are shared with the fixed order result below the peak, and only the first 5 moments are evolved while the remaining moments are held fixed (within the accuracy of the distorted Gaussian approximation). To ensure that the deviation below the peak was not due to the lack of data being fitted there, a fit using all data for which $\xi < \ln(\sqrt{s}/20.5\ {\rm GeV})$ was performed, giving a bad fit everywhere.

TABLE III: Simultaneous fit of N, $\overline{\xi}$, σ^2, s, k, κ_5, κ_6 and $\Lambda_{\rm QCD}$ to TASSO data at 14 GeV and OPAL data at 91 and 202 GeV, with only the first 3 moments evolved according to the MLLA. $\chi^2_{\rm DF} = 1.14$.

N	$\overline{\xi}$	σ^2	s	k	κ_5	κ_6	$\Lambda_{\rm QCD}$ (MeV)
10.90	2.40	1.05	0.05	0.54	0.09	0.19	66 ± 10

TABLE IV: As in Table III, but with only the first 5 moments evolved according to the MLLA. $\chi^2_{\rm DF} = 0.60$.

N	$\overline{\xi}$	σ^2	s	k	κ_5	κ_6	$\Lambda_{\rm QCD}$ (MeV)
10.58	2.15	0.79	-0.79	-0.40	-0.73	-2.44	81 ± 11

In particular since the parameters try to fit to the accurate data below the peak, a large initial $|K_4|$ was obtained.

B. Mellin space parameterization and evolution

We now constrain the initial distribution such that $K_n = 0$ exactly for $n \geq 7$. From Eq. (7), this means that the parameterization of the initial distribution in Mellin space must take the form

$$\ln D_\omega(Q_0) = \sum_{n=0}^{6} \frac{K_p(Q_0)(-\omega)^n}{n!}. \tag{28}$$

We perform fits to TASSO data at 14 GeV and OPAL data at 91 and 202 GeV, cut according to Eq. (26), and evolve according to Eq. (12) with $Q_0 = 14/2$ GeV. Taking $M = 2$, 4 and 6, we obtain the results shown in Tables III, IV and V respectively. Note that using $M = 4$ gives the lowest $\chi^2_{\rm DF}$. For the case $M = 6$, we get a large result for κ_6, since although $\Delta K_6(\alpha_s(Q), \alpha_s(Q_0))$ becomes positive for $Q \to \infty$, for the data used ΔK_6 is negative. This is due to the MLLA term being larger than the DLA term, so it may be the case that corrections beyond the MLLA are required for this quantity, or some other approach. At any rate, from the end of Section II, ΔK_6 contributes spurious higher order terms and should be neglected, and this is confirmed in Table V.

TABLE V: As in Table III, but with only the first 7 moments evolved according to the MLLA. $\chi^2_{\rm DF} = 0.77$.

N	$\overline{\xi}$	σ^2	s	k	κ_5	κ_6	$\Lambda_{\rm QCD}$ (MeV)
10.06	1.80	0.474	-4.86	2.00	-1.17	113.57	96 ± 1

TABLE VI: Simultaneous fit of N', $\overline{\xi}'$, σ'^2, s', k' and $\Lambda_{\rm QCD}$ to TASSO data at 14 GeV and OPAL data at 91 and 202 GeV, with only the first 3 moments evolved according to the MLLA. $\chi^2_{\rm DF} = 1.67$.

N'	$\overline{\xi}'$	σ'^2	s'	k'	$\Lambda_{\rm QCD}$ (MeV)
10.51	2.22	1.17	-0.71	1.18	86 ± 1

C. Distorted Gaussian with Mellin space evolution

In global analyses, the initial FF's are parameterized in x, and the parameters are fitted to data by evolving the FF's in Mellin space in the fixed order approach. For this reason, in [8] the initial gluon FF was parameterized as a distorted Gaussian and evolved using the approach of Eqs. (2) to (4). We repeat this approach here, but instead we will apply MLLA evolution in the form of Eq. (12). First we repeat the fits of Subsection III B. The results for the case $M = 2$ and $M = 4$ are shown in Tables VI and VII respectively. Note again that using $M = 4$ gives the best fit. The resulting curves for the $M = 4$ case are shown in Fig. 3. The cases $M = 6$ cannot be tested since, as we found in Subsection III B, ΔK_6 is negative for the data used so that the integral for the inverse Mellin transform does not converge. Fits in which data for all ξ is used generally give a bad fit everywhere except at values of ξ beyond the peak, which is due in part to the high accuracy of the data at small ξ. As anticipated from the fit of Table II, excellent agreement is found around and above the peak region.

We now perform a fit to all the data, using $M = 4$ in the evolution. The results are shown in Table VIII and Fig. 4, and are the main results of this paper.

In all our approaches, reasonably consistent values of $\Lambda_{\rm QCD}$ were obtained of around 100 MeV. The small ξ region was generally not well described, however this region is outside the scope of the MLLA and requires fixed order corrections. It is generally found that the

TABLE VII: As in Table VI, but with only the first 5 moments evolved according to the MLLA. $\chi^2_{\rm DF} = 0.65$.

N'	$\overline{\xi}'$	σ'^2	s'	k'	$\Lambda_{\rm QCD}$ (MeV)
10.75	2.12	0.92	-0.65	-0.22	77 ± 10

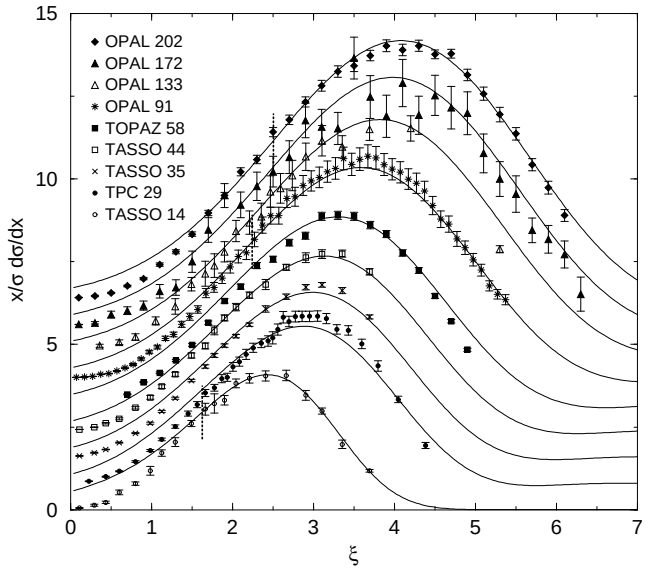

FIG. 3: Fit of the distorted Gaussian parameters and $\Lambda_{\rm QCD}$ to TASSO data at 14 GeV and OPAL data at 91 and 202 GeV, with only the first 5 moments evolved according to the MLLA.

best fit is obtained with $M = 4$, although with other values of M we also obtained good fits around and above the peak.

IV. THE LPHD AND LIMITING SPECTRUM LIMITS

From Eq. (11), $\Delta K_n(\alpha_s(Q), \alpha_s(Q_0)) \to \infty$ as $Q \to \infty$, so that for sufficiently large Q the initial $K_n(Q_0)$ in Eq. (9) may be neglected. However, such an approximation should not be

TABLE VIII: Global fit with only the first 5 moments evolved according to the MLLA. $\chi^2_{\rm DF} = 2.7$.

N'	$\overline{\xi}'$	σ'^2	s'	k'	$\Lambda_{\rm QCD}$ (MeV)
10.39	1.90	1.10	-1.45	-0.09	114 ± 6

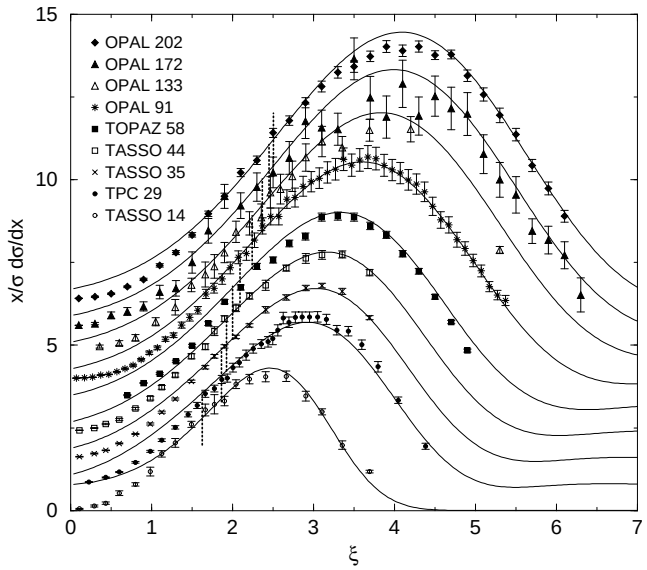

FIG. 4: Global fit with only the first 5 moments evolved according to the MLLA.

made for $n = 0$, since the cross section is very sensitive to the initial $\ln N$. Therefore, data at sufficiently large Q should be reasonably well described with a starting distribution of the form $xD(x, Q_0) = N\delta(1 - x)$. Thus, from a purely perturbative analysis, we see that the LPHD arises because the perturbative components form the dominant contribution to the cross section. In this sense, the LPHD follows from the MLLA rather than being an additional assumption.

For sufficiently large Q, any term of $O(\alpha_s^{-n}(Q_0))$ with n positive can be neglected relative to a term of $O(\alpha_s^{-n}(Q))$, so that from Eq. (11), we may replace $\Delta K_n(\alpha_s(Q), \alpha_s(Q_0))$ with $\Delta K_n(\alpha_s(Q), \infty)$. This can be artificially achieved by setting $Q_0 = \Lambda_{\rm QCD}$, since then $\alpha_s(Q_0) = \infty$ as a consequence of the perturbative approximation. Thus the Limiting Spectrum also follows from the MLLA. However, it is important to note that the $\Delta K_n(\alpha_s(Q), \infty)$ for n sufficiently small would not be finite if corrections of next-to-MLLA or higher were included.

To summarize, a simple analysis of the MLLA shows that, at sufficiently large Q, the assumptions of the LPHD and the Limiting Spectrum will appear to be correct, since the cross section may be calculated with Eq. (9) approximated for $n \geq 1$ by

$$K_n(Q) \approx \Delta K_n(\alpha_s(Q), \infty). \tag{29}$$

To properly test the physical assumptions which imply the LPHD and the Limiting Spectrum requires a comparison with data in the region $Q = O(\Lambda_{\rm QCD})$. However, the only essential difference between our procedure and that of the LPHD with the Limiting Spectrum is

that we do not allow for any assumptions on the size of the initial $\overline{\xi}$ and σ^2, we only assume that the initial κ_n are small. We now study what the effects of these additional constraints are, by using Eq. (29) for $n \geq 1$. From Eq. (9), the normalization $N(Q)$ obeys $\ln N(Q) = \ln \overline{N} + \Delta K_0(\alpha_s(Q), \infty)$, where $\ln \overline{N} = \ln N(Q_0) - \Delta K_0(\alpha_s(Q_0), \infty)$ is independent of Q_0. Thus our predictions will be exactly independent of Q_0, and the theory contains just two free parameters, $\overline{N}$ and $\Lambda_{\rm QCD}$, which we fit to all available data. We find that the data above the cut is best described when the cut is chosen as in Eq. (26) but with $\Delta\xi = +1$ added to the right hand side. Fitting a different normalization for each $\sqrt{s}$ of the data does not improve the fit significantly. For $M = 4$ in the evolution, we obtain $\overline{N} = 7.68 \pm 0.02$, $\Lambda_{\rm QCD} = 446 \pm 2$ and $\chi^2_{\rm DF} = 9.3$, while for $M = 2$ we obtain $\overline{N} = 6.64 \pm 0.02$, $\Lambda_{\rm QCD} = 292 \pm 1$ GeV and $\chi^2_{\rm DF} = 3.74$. The resulting plots are shown in Fig. 5 for the $M = 2$ case. (The $M = 4$ fit gives similar curves.) With these results we are able to calculate the moments at $Q = 14/2$ GeV, and find reasonable agreement with our previous results for N, $\overline{\xi}$ and σ^2 (e.g. that of Table VIII). The evolution of these quantities follows the data, as is to be expected since we are using the same evolution as we used in the fit of, e.g., Table VIII. However, it is clear that the prediction at and below the peak is significantly dependent on the initial values of ξ and σ. Comparing with other analyses which use the LPHD with the Limiting Spectrum, we see that the data above the peak are well described, with no modifications to the normalization, while the data below the peak are not.

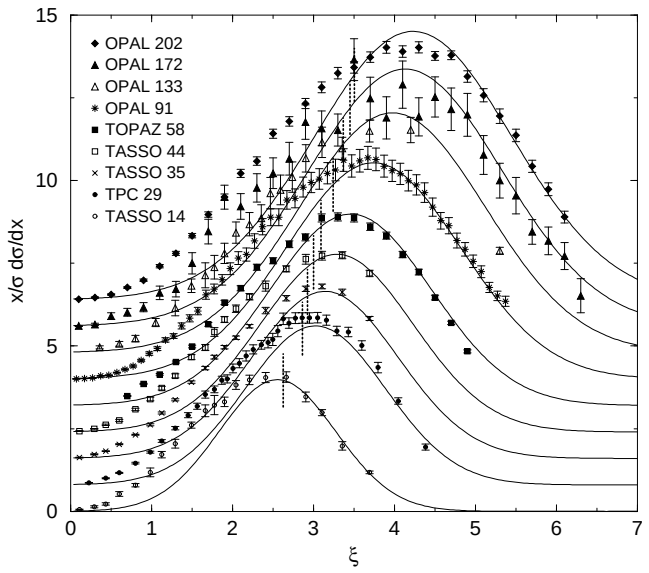

FIG. 5: Global fit to data with the LPHD and Limiting Spectrum, and with only the first 3 moments evolved.

V. CONCLUSIONS

In [8], it was shown that a naive application of the MLLA without additional assumptions gives a good description of data around the peak region, but not beyond. Since the evolution used approached a constant at large $|\omega|$, while the fixed order approach implies that the evolution falls to zero, the contribution to the cross section at large ξ from the cross section at small $|\omega|$ was underestimated. This qualitative feature of the fixed order approach can be taken into account by using the Limiting Spectrum, which decreases fast at large $|\omega|$. In this paper, we found that this feature can also be taken into acount by suppressing the evolution of the higher moments. This does not affect the approximation since, by studying the MLLA in x space, one can see that it is formally justified to neglect their evolution in the perturbative approximation. In addition, at sufficiently large Q, one finds from the MLLA that the spectrum acquires a distorted Gaussian shape. Fixing the higher moments and using a distorted Gaussian for the initial distribution at $Q_0 = 14/2$ GeV resulted in a good description of all data for which $\sqrt{s} \geq 14$ GeV from just below the peak to the largest value of ξ, and one obtains $\Lambda_{\rm QCD} \approx 100$ GeV. In obtaining these results, we used a non-perturbative input that was determined empirically at a low scale, rather than from physical arguments such as those of the LPHD.

Furthermore, we showed that the cross section approaches that of the Limiting Spectrum at sufficiently large Q. We stress that this follows from the MLLA, without additional hypotheses. In practice, imposing the Limiting Spectrum limit on the evolution with suppressed moments and imposing the LPHD on the initial distribution gives a poor description up to the peak. However, a good description is obtained beyond the peak without requiring any modification to the normalization, and the best fit, where $M = 2$, resulted in $\Lambda_{\rm QCD} = 292$ GeV, which is consistent with other analyses.

Finally, the region of the data used in global fits may be extended to lower values of x (large ξ) by incorporating the MLLA into the fixed order calculations. This would allow for a better determination of the FF's, particularly at small momentum fractions, as well as more constraints on $\Lambda_{\rm QCD}$.

Acknowledgments

The authors would like to thank Wolfgang Ochs for helpful suggestions. This work was supported in part by the Deutsche Forschungsgemeinschaft through Grant No. KN 365/1-2, by the Bundesministerium für Bildung und Forschung through Grant No. 05 HT4GUA/4, and by Sun Microsystems through Academic Equipment Grant No. EDUD-7832-000332-GER.

---

[1] Y. L. Dokshitzer and S. I. Troian, Proc. 19th Winter School of the LNPI, Vol. 1, p. 144 (Leningrad, 1984); Y. L. Dokshitzer and S. I. Troian, LNPI-922 preprint (1984); A. H. Mueller, Nucl. Phys. **B213**, 85 (1983), ibid. **B241**, 141 (1984)

[2] Yu. L. Dokshitzer *et al.*, Basics of Perturbative QCD (Editions Frontières, Gif-sur-Yvette, 1991)

[3] V. A. Khoze and W. Ochs, Int. J. Mod. Phys. **A12**, 2949 (1997)

[4] Y. L. Dokshitzer, V. A. Khoze and S. I. Troian, Int. J. Mod. Phys. **A7**, 1875 (1992)

[5] Y. I. Azimov, Y. L. Dokshitzer, V. A. Khoze and S. I. Troian, Z. Phys. **C27**, 65 (1985)

[6] S. Lupia and W. Ochs, Eur. Phys. J. **C2**, 307 (1998)

[7] OPAL, G. Abbiendi *et al.*, Eur. Phys. J. **C27**, 467 (2003)

[8] S. Albino, B. A. Kniehl, G. Kramer and W. Ochs, Eur. Phys. J. **C36**, 49 (2004)

[9] C. P. Fong and B. R. Webber, Phys. Lett. **B229**, 289 (1989)

[10] TASSO, W. Braunschweig *et al.*, Z. Phys. **C47**, 187 (1990)

[11] TPC/Two Gamma, H. Aihara *et al.*, Phys. Rev. Lett. **61**, 1263 (1988)

[12] A. Petersen *et al.*, Phys. Rev. **D37**, 1 (1988)

[13] TOPAZ, R. Itoh *et al.*, Phys. Lett. **B345**, 335 (1995)

[14] ALEPH, R. Barate *et al.*, Phys. Rept. **294**, 1 (1998)

[15] DELPHI, P. Abreu *et al.*, Z. Phys. **C73**, 11 (1996)

[16] L3, B. Adeva *et al.*, Phys. Lett. **B259**, 199 (1991)

[17] OPAL, M. Z. Akrawy *et al.*, Phys. Lett. **B247**, 617 (1990)

[18] SLD, K. Abe *et al.*, Phys. Rev. **D59**, 052001 (1999)

[19] ALEPH, D. Buskulic *et al.*, Z. Phys. **C73**, 409 (1997)

[20] OPAL, G. Alexander *et al.*, Z. Phys. **C72**, 191 (1996)

[21] OPAL, K. Ackerstaff *et al.*, Z. Phys. **C75**, 193 (1997)

[22] OPAL, G. Abbiendi *et al.*, Eur. Phys. J. **C16**, 185 (2000)